CCFE
CULHAM CENTRE FOR FUSION ENERGY

UK Atomic Energy Authority

UKAEA-CCFE-PR(19)65

Allah Rakha, M.J. Mantsinen, A.V. Melnikov, S.E. Sharapov, D.A. Spong, A. Lopez-Fraguas, F. Castejon

Modelling of Alfven cascade modes in stellarator plasmas

Modelling of Alfven cascade modes in stellarator plasmas

Allah Rakha, M.J. Mantsinen, A.V. Melnikov, S.E. Sharapov, D.A. Spong, A. Lopez-Fraguas, F. Castejon

This is a preprint of a paper submitted for publication in Nuclear Fusion

Modelling of Alfvén cascade modes in stellarator plasmas

Allah Rakha[1*], M.J. Mantsinen [1,2], A.V. Melnikov [3,4], S.E. Sharapov[5], D.A. Spong[6], A. López-Fraguas[7], F. Castejón[7]

[1] Barcelona Supercomputing Center, 08034, Barcelona, Spain
[2] ICREA, Pg. Lluís Companys 23, 08010 Barcelona, Spain
[3] National Research Center 'Kurchatov Institute', 123182, Moscow, Russia
[4] Moscow Institute of Physics and Technology (State University) 141700, Dolgoprudny, Russia
[5] National Research Nuclear University MEPhI, 115409, Moscow, Russian Federation
[6] CCFE, Culham Science Centre, Abingdon, OX14 3DB, UK
[7] Oak Ridge National Laboratory, TN, 37831, USA
[8] Fusion National Laboratory, CIEMAT, 28040, Madrid, Spain

E-mail: allah.rakha@bsc.es

May 2019

Abstract.

Alfvén frequency sweeping modes in stellarator plasmas with normal and reversed-shear rotational transform are modelled using a reduced MHD model. We focus on a TJ-II dynamic discharge in which a sequence of frequency sweeping modes with a frequency sweeping range from 20 kHz to 140 kHz (Melnikov A.V. *et al* 2014 *Nucl. Fusion* **54** 123002) have been observed. We find that for the normal shear iota profile a lower number of modes are present centred around 150 kHz of frequency while for radially extended low shear non-monotonic (NM) iota profiles, an extended spectrum of Alfvénic modes is present covering a wider range of frequency from 115 to 295 kHz. Similarly, large number of discrete modes appear for relatively strong negative shear NM iota profiles having frequency range from 36 to 216 kHz. Results for the NM iota profiles with protracted discrete modes are in agreement with the extended frequency sweeping experimental findings. With strong negative shear one of the prominent modes (m = 7, n = 10/11) becomes narrower in radial width. An iota profile with strong negative shear and lower ι_{min} can therefore be considered more favourable for the Alfvén eigenmodes (AEs) stability. **Comparison of this mode's frequencies calculated using standard dispersion relation and modelled through AE3D shows an agreement with the selection of ι_{min} values which supports the MHD spectroscopy calculations.**

Keywords: Reversed-shear Alfvén eigenmodes (RSAEs), Alfvén cascades, Energetic particles (EP) and Stellarator

Submitted to: *Nucl. Fusion*

1. Introduction

Alfvénic instabilities driven by externally generated energetic particles (EPs) for sustainable plasma heating and fusion-born alpha particles are of the primary importance in fusion plasmas. They can deteriorate plasma heating and the confinement of fast particles, cause high heat fluxes on plasma facing components and decrease ignition margin by channelling out the fusion products [1]. Reversed Shear Alfvén eigenmodes (RSAEs), also called Alfvén cascades (ACs) [2–4] are special type of Alfvénic instabilities that arise in the presence of a reversed-shear rotational transform profile. Recently, the interest in reversed magnetic shear plasmas has increased significantly because of the improved confinement conditions with the formation of internal transport barrier (ITB) [5] and magnetohydrodynamics (MHD) stability [6, 7]. In addition, the ACs provide a unique diagnostic opportunity for the experimental estimation of the safety factor (q) profile in tokamaks [8–11] and rotational transform (1/q) also called the iota (ι) profile in stellarator plasmas [12, 13] because of the time evolution of mode frequencies via MHD spectroscopy. MHD spectroscopy provides spectral measurements of the Alfvénic activity and serves as diagnostic tool for the plasma by providing temporal evolution of the safety factor or rotational transform. It has similarity to atomic spectroscopy and helioseismology for the search on internal structure of the sun. Magnetic shear defines the variations in the direction of magnetic field and in the presence of nested flux surfaces it is defined as a radial gradient of the rotational transform. The rotational transform also called an iota profile is defined as the number of poloidal transits per single toroidal transit of a field line on a toroidal magnetic flux surface.

ACs typically exhibit a quasiperiodic pattern of upward or downward frequency sweeping as the local minimum of the inverse safety factor changes in time. Due to the time variation of the iota profile in stellarator plasmas, a rich spectrum of the Alfvénic instabilities has been found. For such instabilities the frequency changes very rapidly in time. This is referred to as frequency sweeping when these rapid variations in frequency are driven by the changes in the equilibrium e.g. changes in the iota profile [14]. In a reverse-shear (RS) configuration, the upward sweep of AC frequency at $q_{min} > m/n$ may approach toroidal Alfvén eigenmode (TAE) frequency as the local minimum of iota drops in time while a downward sweep at $q_{min} < m/n$ can lead to the geodesic acoustic mode (GAM), where $n(m)$ is the toroidal (poloidal) mode number [2]. The ACs resemble Global Alfvén eigenmodes (GAE) since both are cylindrical modes, typically dominated by a single poloidal mode, and since both may exist just below or above the extrema of the shear Alfvén continua. On the contrary, the reverse-shear (RS) modes localize around the extrema of the continua, while the GAEs have radially extended structures [15].

The investigation of EP instabilities is an important goal in three-dimensional (3D) fusion systems since 3D magnetic perturbations are present to some extent in all toroidal magnetic fusion devices with the presence of external symmetry breaking

perturbations [16] and non-axisymmetric effects [17, 18]. As stellarators are inherently 3D fusion devices, investigations and comprehensive understanding of such instabilities in the stellarator plasmas would certainly be beneficial for the future fusion devices. RSAEs have been observed almost in all working fusion devices including stellarators. In Large Helical Device (LHD), RSAEs are observed with non-monotonic rotational transform profile created with counter neutral beam (NB) drive [12]. In TJ-II stellarator the frequency sweeping modes are observed also with the NB injection [19]. Global linear gyrokinetic simulations of the reversed-shear LHD discharges [20] have been used to study their properties. Since the temporal evolution of RSAEs is well described by ideal MHD theory, a reduced MHD model [21] is used to investigate the experimentally observed frequency sweeping phenomena and model their properties over varying ι_{min}. This model solves reduced MHD equations as an eigenvalue problem by ignoring the fast-scale perpendicular dynamics in a 3D toroidal system. Previously, this model has been applied for the modelling of beam-driven EP instabilities in stellarators [20, 23], Reversed Field Pinch (RFP) [24] and tokamaks [14]. Initial modelling results of ACs for the TJ-II stellarator plasmas [25] suggest that the non-monotonic (NM) iota profile supports the experimental observations.

The frequency sweeping modes have been observed in TJ-II stellarator plasmas, and their frequencies have been modelled using a mathematical ansatz for the iota profile as discussed in [19]. Despite of their promising approach and manifestation of following an Alfvénic frequency dependence of plasma density ($1/\sqrt{n_e}$), the fast frequency sweeping of the observed modes remains unexplored. In this paper, we model the observed frequency sweeping modes in TJ-II. These modelling results using this approach of NM iota profile confirm the Alfvénic behavior of observed modes and also associated frequency sweeping phenomenon. We provide modelling results of AEs with normal, radially extended low shear NM iota profiles and further extension with the strong shear centre localized NM iota profiles. The existence of large number of modes with frequencies higher than GAEs and radially well localized mode structures in the presence of NM iota profiles support the experimental observations of frequency sweeping.

This paper is organized as follows. In section 2 the experimental results for TJ-II plasmas with frequency sweeping modes are provided. Section 3 provides a succinct overview of the reduced mathematical model by describing the continuum solver STELLGAP for Alfvén continua and AE3D code for the modes analysis. The section 4 describes an equilibrium reconstruction for the modeled iota profiles. In section 5, simulation results for both the Alfvén continuum and mode structures are discussed, and section 6 gives a summary and conclusions of the findings.

2. Experimental Observations

TJ-II is a four-field period flexible heliac with a major radius $R = 1.5$ m, an averaged minor radius $\bar{a} \leq 0.22$ m, and an equilibrium magnetic field of $B_0 = 0.95$ T. Experiments have been performed at TJ-II stellarator to investigate the up or down frequency

sweeping of NBI-driven Alfvén eigenmodes by varying the magnetic configuration during a discharge. The magnetic configuration has been linearly varied over a time period of 60 ms by changing currents in helical coils [26]. The variations in iota profile appear due to the variations in plasma current for different reasons (skin current, dynamic configuration and changes in vertical /poloidal field). It has been observed that the changes in the iota profile significantly vary the AE mode frequency, while the mode location does not change much if these variations are relatively small.

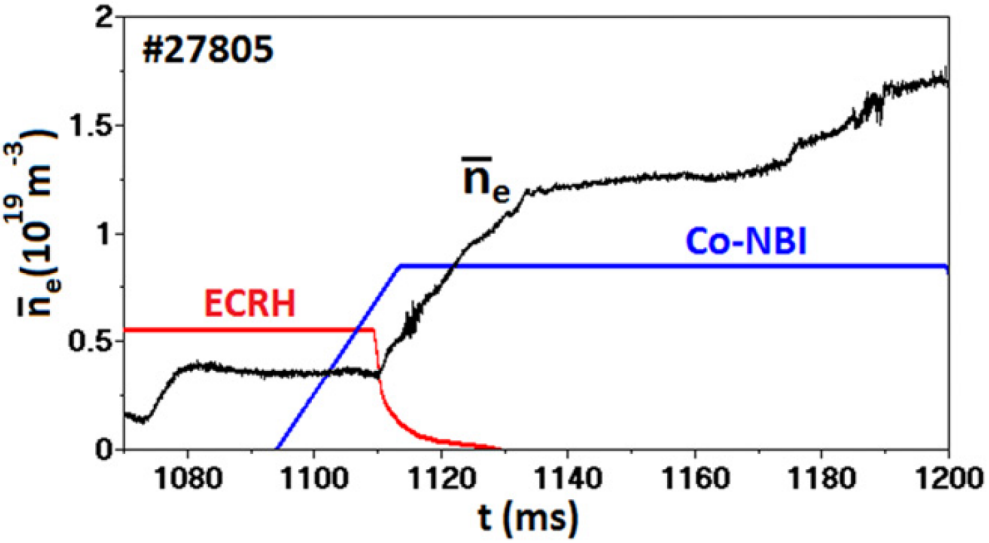

Figure 1: A typical TJ-II discharge scenario and the corresponding line averaged plasma density evolution [19]

A typical TJ-II discharge scenario with the dynamic magnetic configuration is shown in Figure 1 [19]. In this scenario, at the first plasma is created and heated with an off-axis electron-cyclotron resonance heating (ECRH) and in the subsequent part the plasma is heated with the neutral beam injection (NBI) only. After switching-off the ECRH, the plasma is sustained only with NBI heating, which also increases the plasma density.

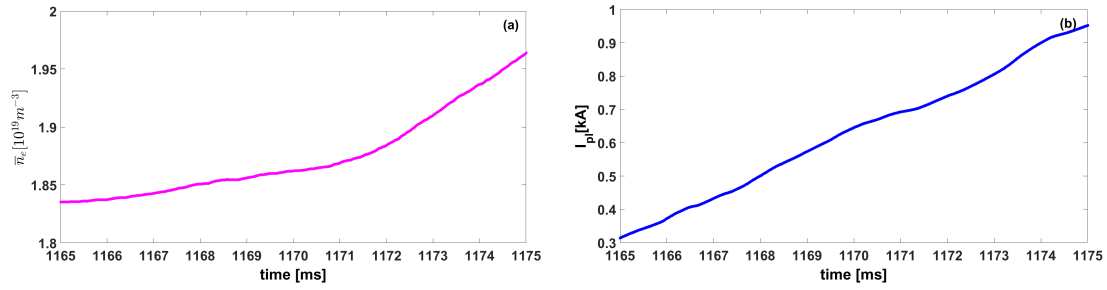

Figure 2: Temporal evolution of (a) the plasma density and (b) current for TJ-II discharge #27804

We focus in our analysis on TJ-II discharge 27804 where an Alfvénic activity has

been observed with downwards frequency sweeping at t = 1165-70 ms. The frequency sweeping modes are clearly visible in the plasma density spectrogram shown in Figure 3. The range of this fast downward frequency sweeping is from 150 kHz to 25 kHz in the time span of only $\sim$ 10 ms. This observed sharp frequency sweeping at nearly constant line averaged density $\bar{n_e} = 1.8 \times 10^{19} m^{-3}$ from t = 1165 to 1170 ms (Figure 2a) is expected because of the variations in iota profile induced through the relatively small variation in plasmas current (Figure 2b). The cross-coherence of Heavy Ion Beam Probe (HIBP) and bolometer signals shows that the observed modes are radially extended and they are located around ($\rho \approx 0.7$). Here, ρ is a radial parameter which is defined as $\rho = \sqrt{\psi_t}$, where ψ_t is normalized toroidal flux.

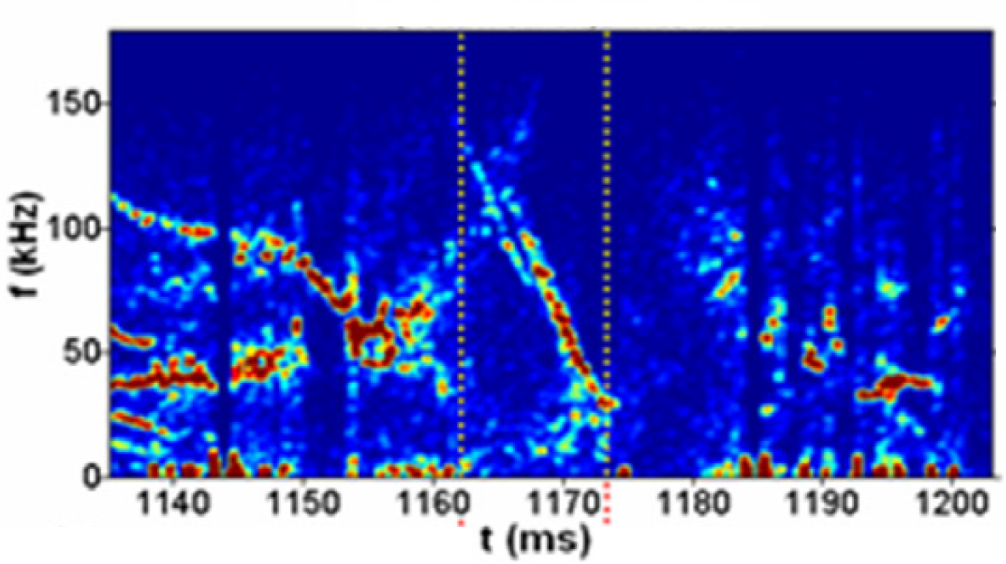

Figure 3: Plasma density spectrogram measured by HIBP for TJ-II discharge #27804 [19]

In discharge 27804, the temporal evolution of plasma current shows finite variations during the time window ($\sim$ 10 ms) of mode sweeping as shown in Figure 2. These variations are $\Delta I_p = 0.35$ kA from t = 1165 to 1170 ms which can contribute to the details of the mode behaviour. Experimentally their effects on the modes evolution have been studied in detail in reference [19]. In order to correctly model the experimental results we have carefully employed the experimental plasma density and current or iota profiles in our modelling calculations.

3. Mathematical model

We use the reduced MHD model (RMHD) [21] to model TJ-II discharge 27804. A brief description of the RMHD model [21] is provided in this section. In the reduced MHD model, full MHD equations are transformed into a reduced set of MHD equations by using wavelength ordering. In wavelength ordering, the perpendicular wavelength of a

perturbation is considered smaller than its parallel wavelength i.e. $\lambda_\perp/\lambda_\parallel \sim \epsilon$ and $\epsilon \ll 1$ which serves an expansion parameter. This wavelength ordering is defined for directions relative to a large-scale magnetic field. Since this set of reduced MHD equations is derived without using aspect ratio ordering, it can be applied on any general toroidal configuration. In this model the zeroth-order quantities satisfy an equilibrium equation and do not vary with time. This is because the expansion parameter (ϵ) has been defined by the anisotropy of the perturbed response. Consequently no assumptions are made on the zeroth-order quantities. Manifesting the MHD equilibrium and setting constraints to eliminate the fast time-scale perpendicular waves, the reduced MHD equations have been formulated for the evolution of scalar potential quantities on the time scales associated with the parallel wave vector (shear-Alfvén wave time scale), which are important for the plasma stability studies. Energy conservation and divergence-free magnetic fields at the higher orders of expansion parameter have also been incorporated.

Based on the RMHD model, a set of numerical tools for the modelling of Alfvénic instabilities in 3D toroidal fusion systems has been developed. For the analysis of shear Alfvén continuum and relevant gap structures, a specific tool i.e. STELLGAP [27] in the incompressible and low β limit is employed in this study. The detailed derivations used in STELLGAP are provided in [28]. The governing equation of STELLGAP for the computation of the continuum structures is given as,

$$\mu_0\rho\omega^2\frac{|\nabla\psi|^2}{B^2}\xi_s + \vec{B}\cdot\vec{\nabla}\{\frac{|\nabla\psi|^2}{B^2}(\vec{B}\cdot\vec{\nabla})\xi_s\} = 0 \tag{1}$$

where the magnetic surface displacement is $\xi_s = \vec{\xi}(\vec{B}\times\vec{\nabla}\psi)/|\nabla\psi|^2$. This equation can be represented for different poloidal (m) and toroidal (n) mode numbers as a symmetric matrix eigenvalue equation,

$$\omega^2 \overleftrightarrow{A}\,\vec{x} \;=\; \overleftrightarrow{B}\,\vec{x} \tag{2}$$

where $\vec{x}$ is a vector having different components of ξ_s. With this set of equations, the Alfvén continuum is computed by STELLGAP for all relevant modes numbers (m, n) using the DGEGV routine from the IBM ESSL library.

For the modes structures investigations, a clustered frequency model [29], i.e. the AE3D code has been employed. AE3D is an eigenvalue code, which calculates Alfvén eigenmodes in 3D equilibria using described above reduced MHD model of shear Alfvén waves for 3D toroidal plasmas. In this reduced system, the two basic laws, i.e. the ideal MHD Ohm's law and the 3D vorticity equations, lead to an eigenvalue problem.

$$\omega^2\nabla\cdot(\frac{1}{{V^2}_A}\nabla\phi) + (\vec{B}\cdot\vec{\nabla})\{\frac{1}{B}\nabla^2(\frac{\vec{B}}{B}\cdot\nabla\phi)\} + \nabla\zeta\times\nabla(\frac{\vec{B}}{B}\cdot\nabla\phi)\cdot\nabla\frac{J_{\parallel 0}}{B} = 0 \tag{3}$$

AE3D can solve the eigenvalue equation (3) fully or partially. While it is time consuming to solve for the full spectrum of modes, a partial solution can be invoked by providing a seed gap frequency around which a cluster of the modes can be found. AE3D achieves faster performance for the partial but sufficient solution by pre-specifying an eigenvalue

(frequency) for the eigenmodes search as a subset of all eigenvalues using a Jacobi-Davidson style QZ (JDQZ) algorithm [30].

4. Equilibrium reconstruction

In the first step, MHD equilibrium calculations have been performed using the experimental magnetic geometry and plasma parameters for TJ-II discharge 27804 at t = 1170 ms with an equilibrium solver VMEC [22]. The VMEC iteratively solves MHD model using a variational method to find a minimum of the system energy for the reconstruction of an equilibrium. It solves the MHD model only for the closed magnetic flux surfaces and, therefore, does not allow any formation of stochastic structures of the magnetic field.

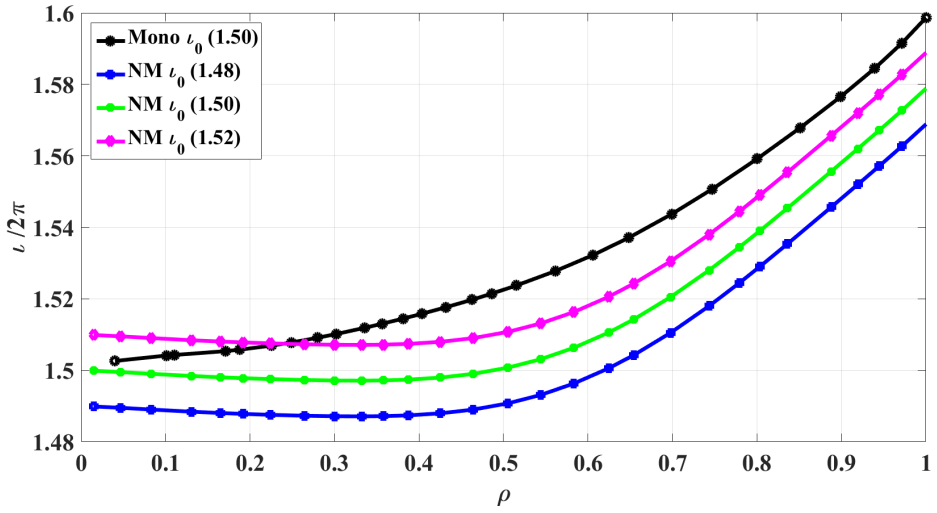

Figure 4: Normal (monotonic) and radially extended low-shear non-monotonic (NM) rotational transform (iota) profiles for TJ-II discharge 27804 with an on-axis iota value of $\iota(0) = 1.50$.

In the TJ-II discharge 27804, for the frequency sweeping modes an on-axis iota value $\iota(0)$ was determined around 1.5 [19]. Therefore, we have considered an on-axis iota of $\iota(0) = 1.50$ for the reconstruction of plasma equilibrium with normal (monotonic) and non-monotonic (NM) iota profiles. For the normal iota profile case, a linear iota profile is considered with $\iota(0) = 1.5$ for the reconstruction of fixed boundary MHD equilibrium to model the experimentally observed frequency sweeping modes. Alfvén continuum and modes analysis given in section 5 with fewer number of modes could not explain the experimentally observed frequency weeping phenomenon. Therefore, we considered reversed shear NM iota profiles with radially extended low shear and centrally localized relatively strong shear regions.

TJ-II fixed-boundary equilibrium with radially extended low-shear NM iota profile is achieved with $\iota(0) = 1.49$, 1.50 and 1.51 (see Figure 4). Extended low shear equilibrium is computed to model a larger core area with the reversed shear. Three

distinct values of $\iota(0)$ are considered to investigate the sensitivity of on axis iota value in the reversed-shear iota profiles for the extended mode analysis. A similar extended low shear region was observed with the neutral beam current drive (NBCD) in Large Helical Device (LHD) [20] populated with the Alfvénic activity. Normal and low-shear NM iota profiles all range between $1.50 \geq \iota/2\pi \leq 1.6$. In these low sheared NM iota profiles, the low shear region radially extends up to $\rho \approx 0.5$ with the minimum located around $\rho \approx 0.4$.

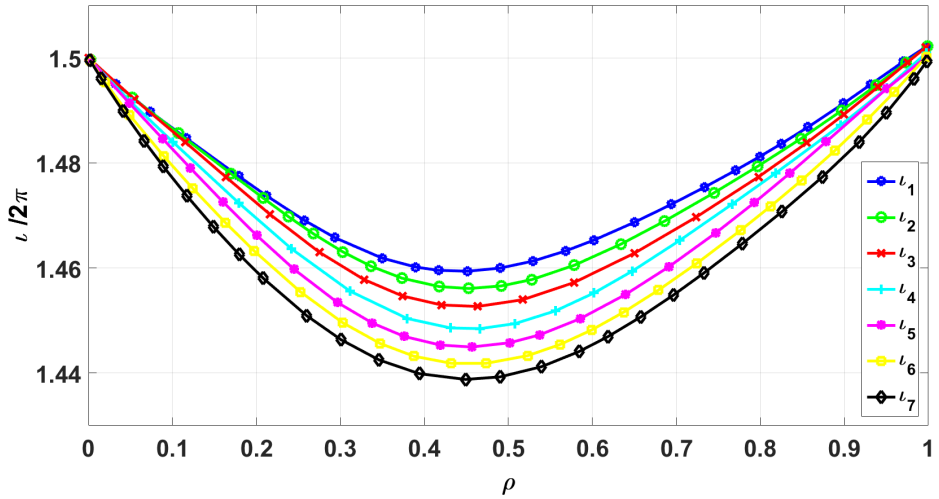

Figure 5: Strong shear non-monotonic (NM) rotational transform (iota) profiles modeled for the TJ-II discharge #27804 with on-axis iota vales $\iota(0) = 1.50$ and varying ι_{min} from 1.4388 to 1.4594 around $\rho = 0.45$ in seven similar profiles.

Table 1: Minimum iota values i.e. ι_{min} for the seven strong shear NM iota profiles

ι_1	ι_2	ι_3	ι_4	ι_5	ι_6	ι_7
1.4594	1.4561	1.4527	1.4485	1.4450	1.4418	1.4388

Similarly, to investigate the strong shear effect, equilibrium calculations are performed by introducing strong shear in the iota profiles and keeping ι_0 and iota edge = 1.5. Seven similar strong shear NM iota profiles with varying ι_{min} shown in Table 1 radially lying around $\rho \approx 0.45$ as shown in Figure 5 are considered to investigate the ι_{min} effect on the modeled modes. This set of strong shear NM iota profiles is considered because of the ι_{min} range shown in Table 1 which remains lower than the 3/2 rational surface. Comparison between the frequencies of modes calculated through AE3D code and using theoretical dispersion relation enables these modelling efforts for the active calculations of ι_{min} in NM iota profiles. These calculations of ι_{min} in NM iota profiles serve as important diagnostic tool for the precise iota values following MHD theory. Experimental parameters of discharge 27804 are employed to reconstruct these fixed-

boundary equilibria, so that these calculations could provide a platform through which a real iota profile could be reconstructed using MHD spectroscopy [8, 11].

5. Simulation results

Following the plasma equilibrium reconstruction, Alfvén continuum spectra for the normal, radially extended low-shear NM and strong shear NM iota profiles are computed using STELLGAP solver [27] and their detailed discussion is provided in section 5.1. The analysis of the Alfvén modes with AE3D [29] code for all three types of iota profiles by computing their radial electrostatic potential profiles is provided in the section 5.2 which describes the nature of the modes, their prominent modes numbers, frequencies and radial localization.

5.1. Alfvén continuum spectra analysis

The observed frequency sweeping Alfvénic modes are modelled using reduced MHD simulations for the normal, low shear NM and strong shear NM iota profiles. In first step, in order to examine possible continuum gaps, the Alfvén continuum structures are calculated using STELLGAP [27]. These continuum calculations provide information on the possible formation of frequency gaps and the likely radial localization of the Alfvén modes at the gaps and extremum points in Alfvén continuum.

Alfvén continuum structures for the normal iota profile are plotted in Figure 6. Figure 6 shows that the gaps form at frequencies of around 185 and 220 kHz and radially lie at ρ is 0.7 and 0.5 respectively. While here are some low-frequency extrema present in these structures, these extrema are subject to the strong continuum damping, which inhibit low-frequency modes. Because of limited gaps the continuum calculated with the normal iota profile are not able to describe the possibility of larger number of modes or modes which extend in frequency range. Calculations with reverse shear NM iota profiles are therefore considered important as the possibility of describing frequency sweeping modes with reverse shear in helical plasmas has been reported [12, 20].

In the first step, for modeling the observed frequency sweeping modes, a radially extended low-shear NM iota profile (Figure 4) is used as similar iota profiles are considered in similar investigations [20]. The corresponding continuum for three similar radially extended low-shear NM iota profiles with different on-axis iota $\iota(0)$ are plotted in Figure 7. The continuum structures that form extremes and gaps in all three continua are extended radially up to $\rho \approx 0.75$ as the corresponding iota profiles are extended. In addition, gaps and extremum points move radially outward and upward in the frequency range as the $\iota(0)$ value increases from 1.49 to 1.51. Particularly, in the case of $\iota(0) = 1.50$ there are two wide gaps, first between 5 kHz to 140 kHz and second between 170 kHz to 290 kHz are important since they provide possibility of modes which may have larger frequency variations. Since normal and one of the low-shear NM iota profiles have $\iota(0) = 1.50$, it seems more reasonable to explain observed frequency sweeping modes with wider continuum gaps with the low shear NM iota profile.

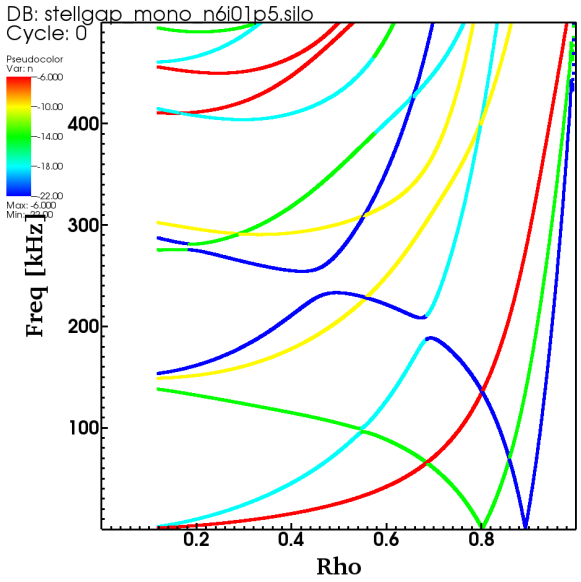

Figure 6: Alfvén continuum structures for the normal/monotonic iota profile for discharge 27804. The color coding of continua represent the corresponding toroidal mode number (n).

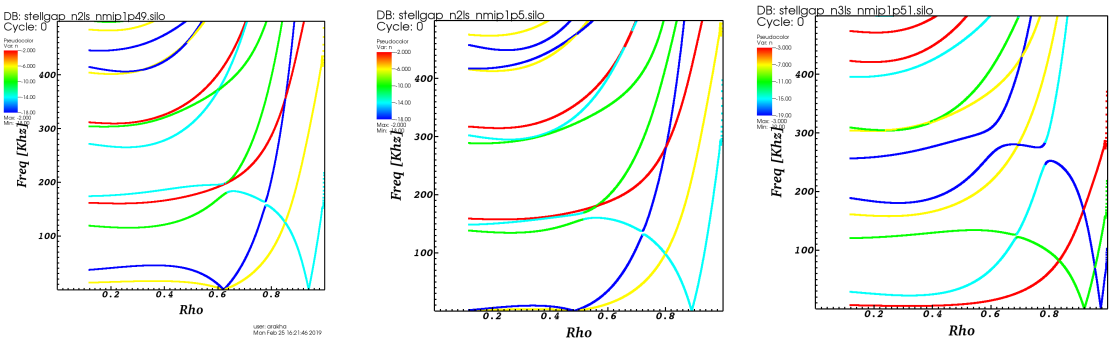

Figure 7: Alfvén continuum structures for the extended low shear NM iota profiles with on-axis values of $\iota(0) = 1.49$, 1.50 and 1.51 from left to right by keeping all other parameters of discharge 27804. The color coding of continua represent the corresponding toroidal mode number (n).

In the second step, Alfvén continua are calculated with varying minimum value ι_{min} for the strong negative shear NM iota profiles (see Figure 5). Variation of the ι_{min} provides an opportunity to model an optimum iota profile scaling with the mode frequency, this diagnostics methodology is referred as MHD spectroscopy principle [8].The continuum structures for three out of seven iota profiles ($\iota 1$, $\iota 4$, and $\iota 7$) from left to right cover significant differences between these continua and show all gap structures in Figure 8. Three important gaps with frequencies in the range of 70-80, 140 and 210 kHz persist in all three continuum structures besides the extremum points. In addition to the persistence of gaps, the gaps are core localized and radially extended up to $\rho \approx$

= 0.6, towards the edge of plasma column the continuum structures do not form any gaps. In these modeled continua a large number of the gaps appear which provide the possibility of describing large frequency range of the observed frequency sweeping modes.

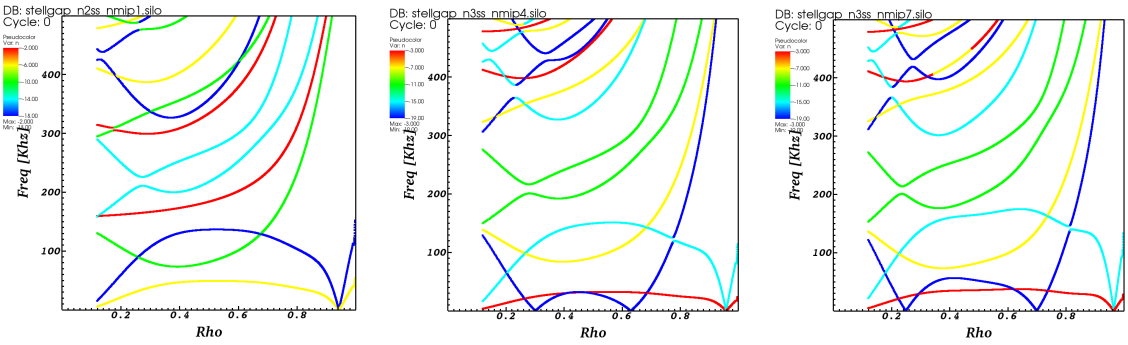

Figure 8: Alfvén continuum structures for the strong shear NM iota profiles with on-axis value $\iota(0) = 1.50$ for the ι_1, ι_4, and ι_7 profiles from left to right by keeping all other parameters of discharge 27804. The color coding of continua represent the corresponding toroidal mode number (n).

The comparison of Alfvén continuum structures shows relatively fewer gaps and extremum points for the normal iota profile, covering a short frequency range and radial extent. While there is a relatively wider spectrum of gaps and extremum points across a wider frequency range and radial extent for both NM iota profiles.

This comparative study also highlights the effect of NM iota profile with the generation of extremum points in the range of low-frequency Alfvén continuum. Comparison between the Alfvén continuum of normal and NM iota profiles shows that the gaps are radially very localized in normal iota profiles whereas in the NM iota profiles the gaps or extemum points are radially extended in the core region of plasma column. These radially localized and /or extended gaps accommodate a large number of modes which support the observed frequency sweeping modes.

5.2. Alfvén modes analysis

In section 5.1, our modelling results of Alfvén continuum for the TJ-II discharge 27804 with normal, low and strong shear NM iota profiles are provided. In this section we provide modes analysis using reduced MHD clustered frequency model (AE3D) for the modeled cases. The mode analysis includes the potential profiles, radial localization, mode frequencies and the combination of prominent toroidal 'n' and poloidal 'm' mode numbers.

Simulations have shown that both in normal and NM low shear iota profiles with on-axis iota $\iota(0) = 1.50$ have some identical modes, their frequencies and radial positions are shown in Figure 9. This analysis shows that the modes are core localized for these iota profiles however they appear higher in number covering a large frequency range for

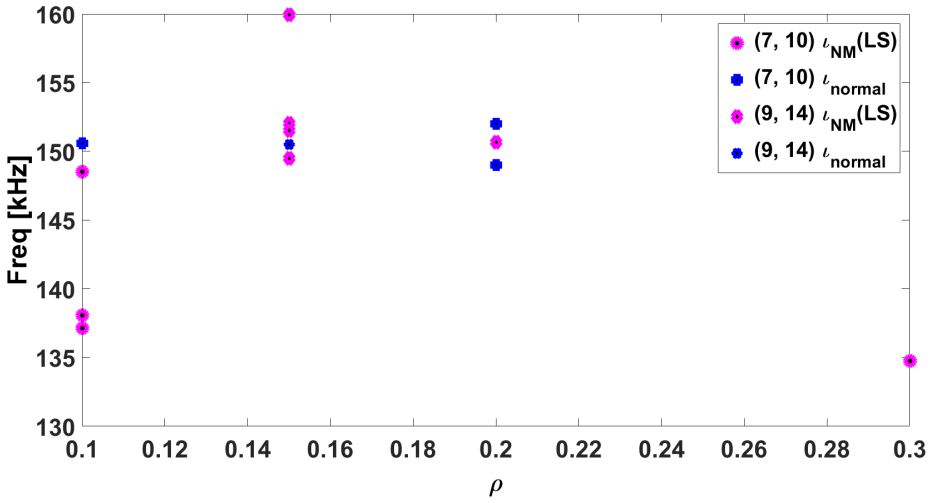

Figure 9: Scatter plot for frequencies and radial locations of the identical modes obtained with the normal and low shear NM iota profiles with on-axis iota $\iota(0) = 1.50$

the low shear NM iota profile. Potential profiles of the modes (m = 7, n = 10) and (m = 9, n = 14) which appear in the both iota profiles are plotted in Figure 10. This shows the modes with low shear NM iota profile are relatively extended radially up to $\rho \approx 0.3$ with frequencies 135 and 149 kHz while for normal iota profile similar modes are present which are radially localized around $\rho \approx 0.1$ and they have frequency of 150 kHz.

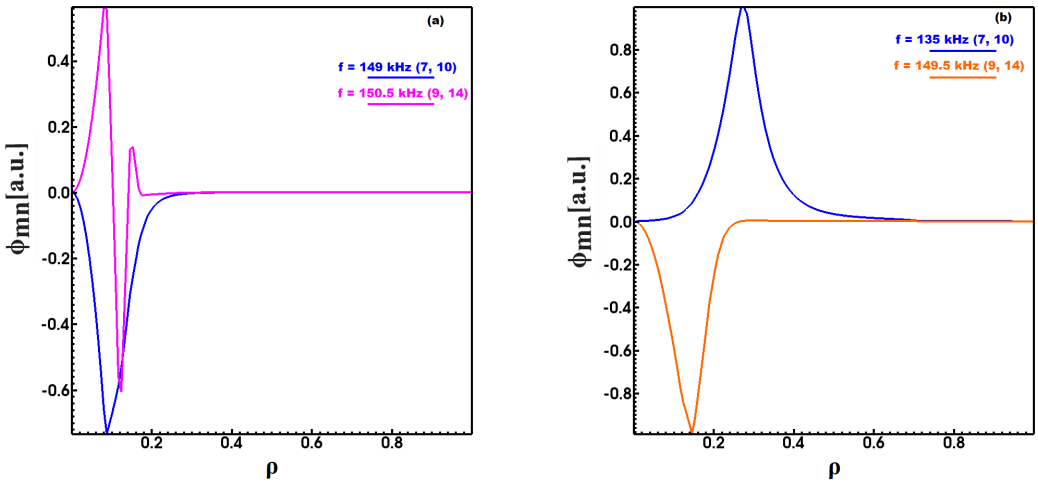

Figure 10: Alfvén modes with the (a) normal and (b) low shear NM iota profiles with on-axis iota $\iota(0) = 1.50$. The corresponding frequencies and prominent mode number pairs (m, n) are shown as legend.

The mode analysis for the three similar low shear NM iota profiles having different $\iota(0)$ is shown in Figures 11,12, and 13. A large number of modes are present in these

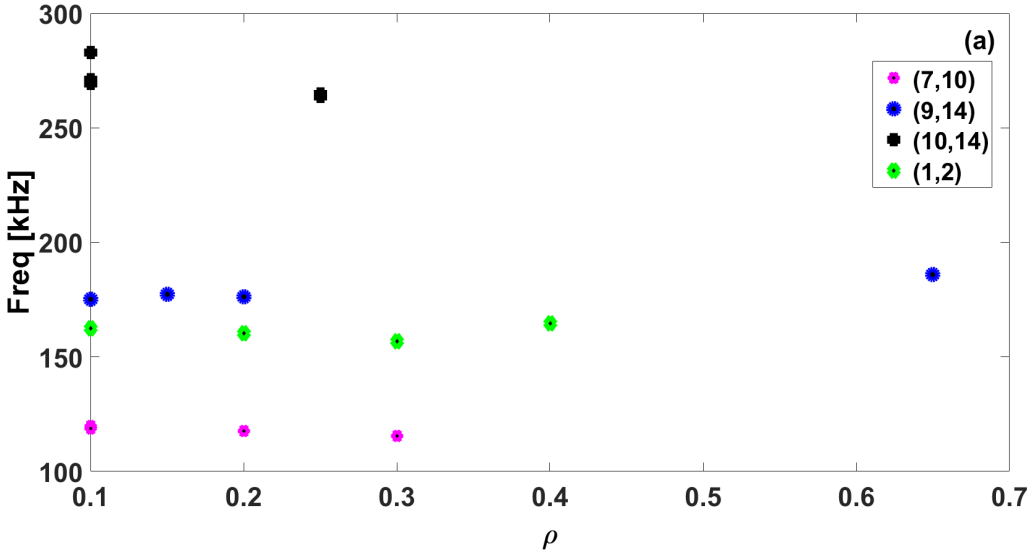

Figure 11: Scatter plots for frequencies and radial locations of the prominent modes obtained with the low shear NM iota profiles with $\iota(0) = 1.49$

low shear NM iota profile cases covering a wide range of radial extent up to $\rho \approx 0.8$ with frequencies up to 300 kHz. The number of modes decrease by the increase in $\iota(0)$ = 1.49 to 1.51. The radial potential profiles of the representative modes are presented in Figure 14. An identical mode (m = 7, n = 10/11) appears for these three similar iota profiles, where for the $\iota(0) = 1.51$ the n = 11 becomes prominent instead of n = 10 because of the selection of n+1 continuum. Qualitatively these modes share identical frequencies, while their radial extents are unique. Most of these modes are dominated by a single poloidal mode by forming structures similar with the GAEs. The modes with lower n i.e. n = 2 are extended over a wider radial extent and the modes with higher n are relatively localized over their radial positions. Modes having properties of single poloidal dominance and their radial localization for the higher n suggest that these modes are reversed shear AEs. One of the modes (m = 7, n = 10/11) which appears in all of three parts have frequencies of 115, 135 and 121 and 135 kHz with radial locations of ρ = 0.25, 0.3 and 0.15 and 0.55 respectively.

After investigating the Alfvénic instabilities for the low-shear NM iota profiles, further investigations with the relatively strong shear NM iota profiles are performed. Seven similar iota profiles with varying ι_{min} having identical shapes and $\iota(0) = 1.50$ are employed to investigate the effect of ι_{min} on the mode analysis. Figures 15, 16 show the frequency of prominent modes with ι_{min} does not vary much, although the finite variations are computed which are an essence of the ι_{min} variations. Results are divided in to two similar sets on the basis of modes which appear in each set, since after ι_4 profile the mode numbers get modified because of the selection of higher n+1 continua for those cases. Results have shown the decrease in the number of the prominent modes with the decrease of ι_{min}.

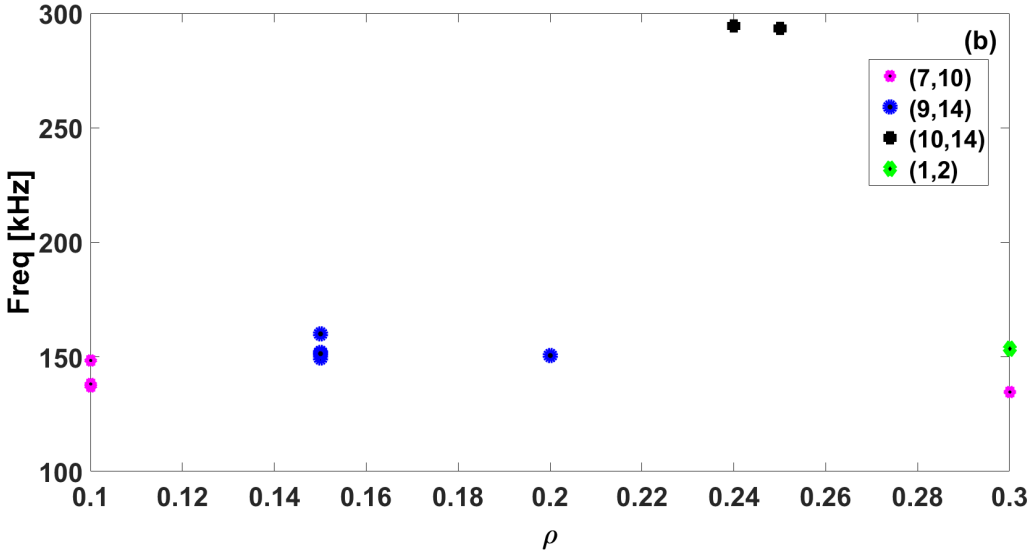

Figure 12: Scatter plots for frequencies and radial locations of the prominent modes obtained with the low shear NM iota profiles with $\iota(0) = 1.50$

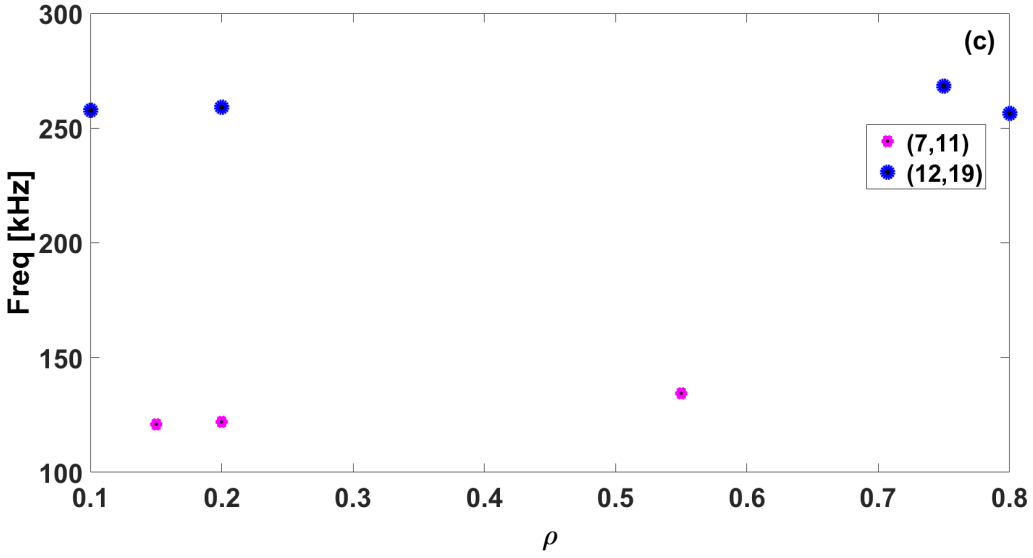

Figure 13: Scatter plots for frequencies and radial locations of the prominent modes obtained with the low shear NM iota profiles with $\iota(0) = 1.51$

The radial mode structures potential profiles of the prominent modes for the relatively strong shear NM iota profiles from ι_1 to ι_3 are plotted in Figure 17. Similar to the low shear NM iota profile case, the modes with relatively strong shear NM iota profiles are also dominated by single poloidal harmonic and radially localized except modes (m = 1, n = 2) and (m = 4, n = 6) which are radially extended over a wide region and characterized as GAEs. Mode (m = 4, n = 6) also seems to go through a transition from GAE to RSAE after getting radially localized ι_3 case. Small fluctuations

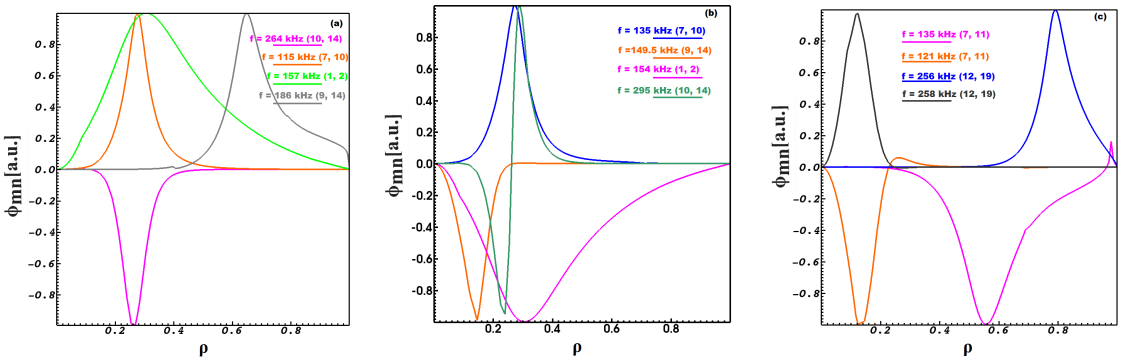

Figure 14: Alfvén modes with the low shear NM iota profiles with $\iota(0)$ = (a) 1.49, (b) 1.50 and (c) 1.51. The corresponding frequencies and prominent mode number pairs (m, n) are shown as legend.

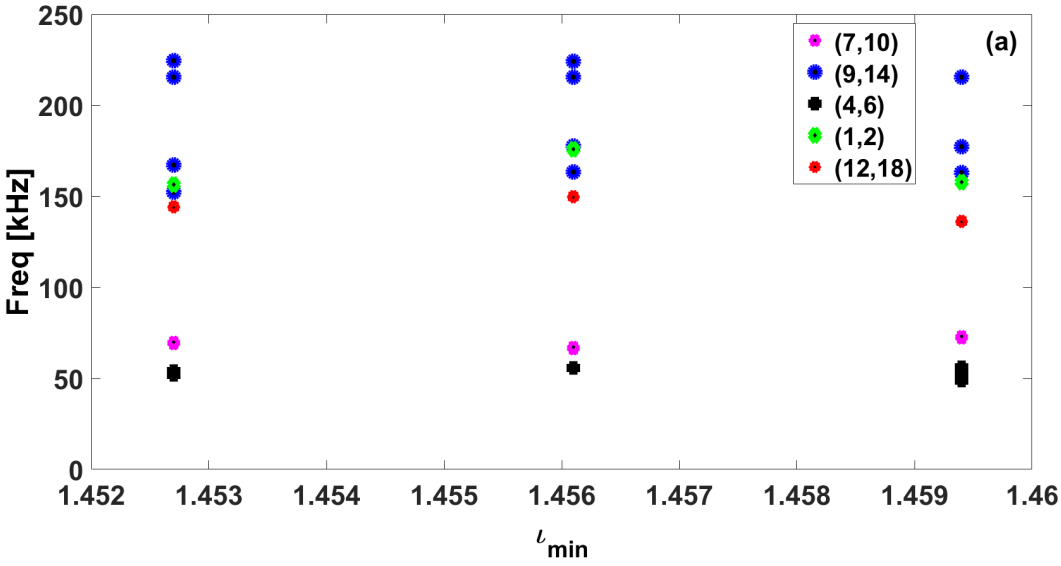

Figure 15: The variation of the frequencies with minimum value of iota ι_{min} of the identical modes obtained with the strong shear NM iota profiles having $\iota(0) = 1.50$ for the iota profiles ι_1 to ι_3 of Figure 5.

in the frequencies of the modes (m = 4, n = 6) and (m = 7, n = 10) are found among ι_1 and ι_3 cases. Most of these modes are radially localized up to $\rho = 0.6$ except the GAEs. These modes cover a range of frequency from 49 to 216 kHz which is roughly consistent with the experimental findings.

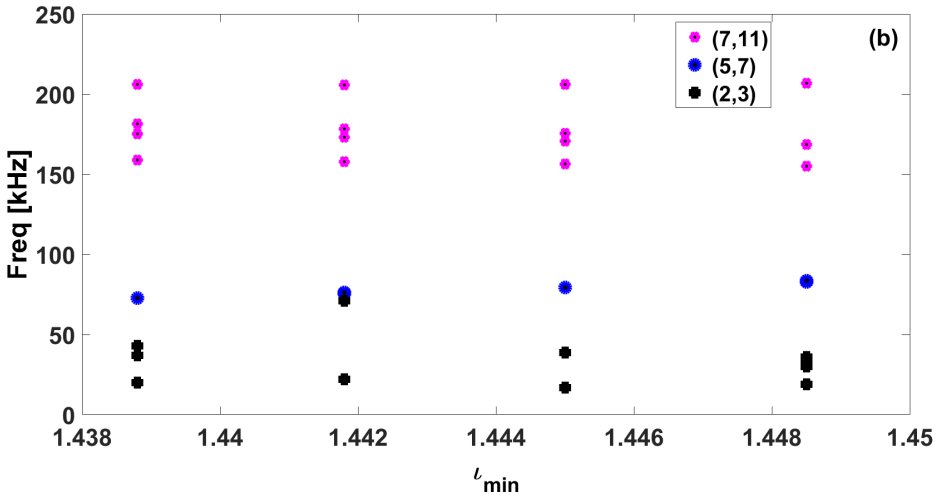

Figure 16: The variation of the frequencies with minimum value of iota ι_{min} of the identical modes obtained with the strong shear NM iota profiles having $\iota(0) = 1.50$ for the iota profiles ι_4 to ι_7 of Figure 5.

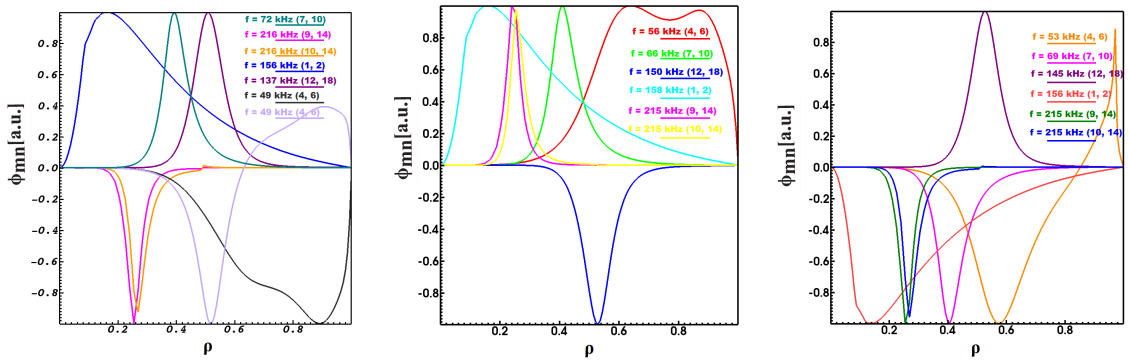

Figure 17: Alfvén eigenmodes (AEs) radial structures for the NM iota profiles (a) ι_1 with $\iota_{min} = 1.4594$ (b) ι_2 with $\iota_{min} = 1.4561$ and (c) ι_3 with $\iota_{min} = 1.4527$. The corresponding frequencies and prominent mode number pairs (m, n) are shown as legend.

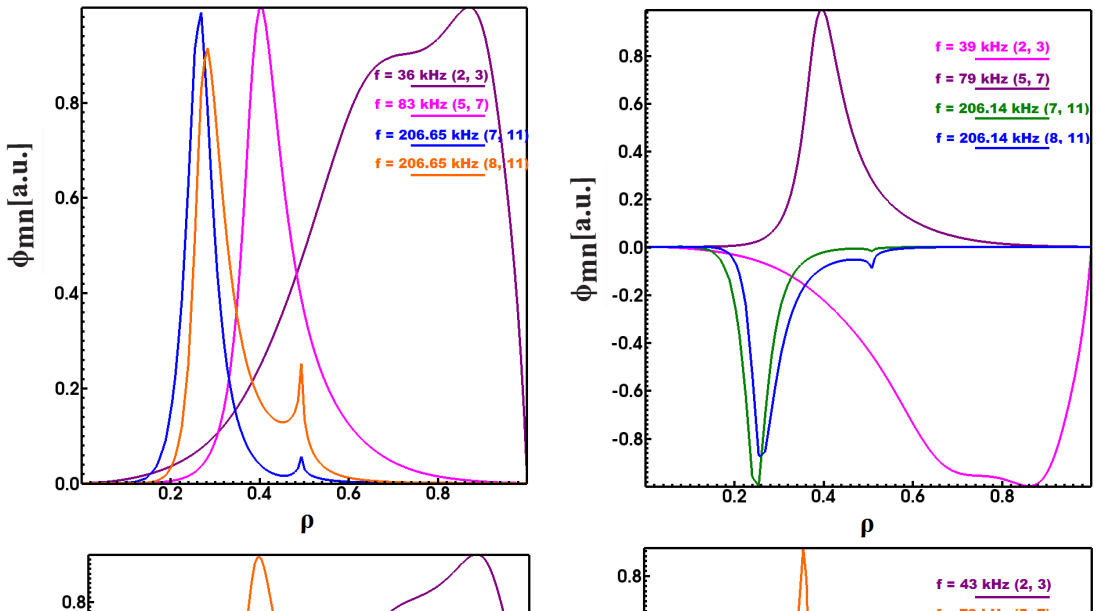

The potential profiles forming radial mode structures for the second set of the strong shear NM iota profiles results from ι_4 to ι_7 are plotted in Figure 18. There are four prominent modes covering a wide range of frequencies from 36 to 206.65 kHz. Three of these modes which are radially localized around $\rho = 0.4$, their frequency decreases with the decrease of ι_{min} are characterized as RSAEs and one of them (m = 2, n = 3), which is radially extended over a wider extent up to $\rho = 0.9$ increases in frequency from 36 to 43 kHz with the decrease in ι_{min} is characterised as GAE.

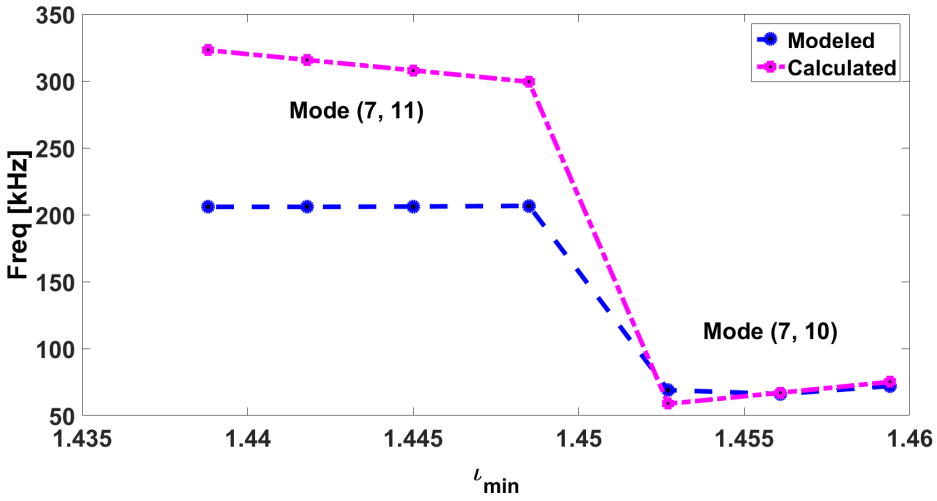

Figure 19: Variation of the modeled frequency (using AE3D code) of the mode with ι_{min} and its comparison with the calculated mode frequency (using analytical dispersion relation).

The frequency analysis of the modes (m = 7, n = 10/11) with the variation of the ι_{min} is plotted in Figure 19. This shows for the both modes (m = 7, n = 10/11), the frequencies calculated with the dispersion relation of the shear Alfvén waves using ι_{min} values and modeled through the reduced MHD model by using strong shear NM iota profiles are consistent. There are differences at low ι_{min} values between the frequencies of modeled and calculated modes, since in these calculations we have focused on the lower frequencies of the modes and have discarded the calculations of the higher frequency modes therefore, these differences can be accepted for this comparison. **This comparison provides an active diagnostic tool for the ι_{min} calculations in the fusion plasmas.**

The radial width of the identical modes (m = 7, n = 10/11) is also calculated and its variation with the ι_{min} is plotted in Figure 20. This shows the radial width of these modes increases with the increase of ι_{min} values, which means that the strong shear drives the modes more narrower and radially well localized. The narrower modes due to low region of interaction with fast ions do not drive energetic particles radially. Therefore, strong shear NM iota profiles with lower ι_{min} are considered favourable for the AEs stability.

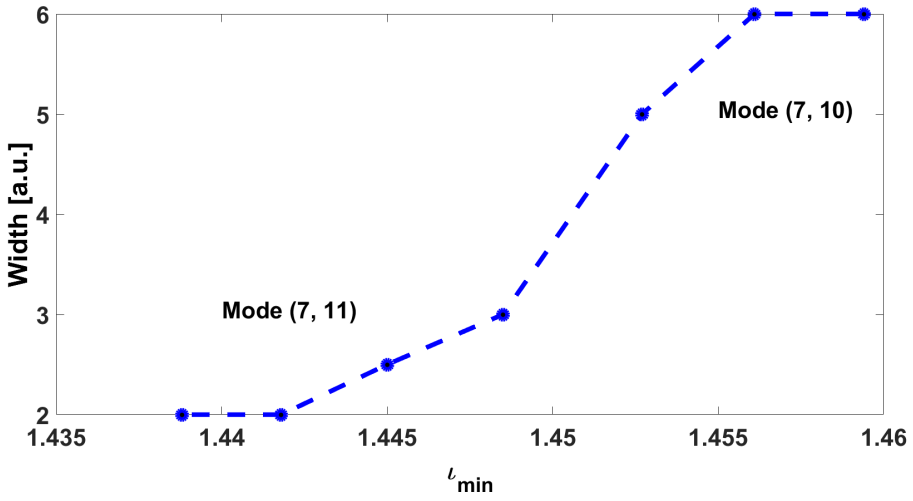

Figure 20: Variation of the mode width calculated as FWHM of mode amplitude with ι_{min}

6. Summary and conclusions

Detailed analysis of the Alfvénic instabilities has been performed using STELLGAP and AE3D codes for the three different types of rotational transform profiles in the low-field and low density TJ-II stellarator plasmas where the Alfvénic activity with frequency sweeping was observed [19]. In the comparison of the results of normal and radially extended low shear NM iota profiles, two similar core localized modes (m = 7, n = 10) and (m = 9, n = 14) appear with discrete frequencies. The frequency range of the modes calculated using low shear NM iota profile covers from 135 to 150 kHz and is relatively larger than the normal iota profile for which these modes are centred around 150 kHz. This shows the results obtained using low shear NM iota profile explain better the frequency sweeping experimental observations.

Finite variations of the on-axis iota value with shifted iota profiles have found a variety of Alfvén modes covering a similar wide frequency range from 115 to 295 kHz. Radially extended GAE and localized RSAEs are identified in these calculations covering a radial range up to $\rho = 0.6$. Radially localized RSAE mode (m = 7, n = 10/11) appears with the frequencies of 115, 135 and 121 kHz and radial localization around $\rho = 0.3$ and 0.15 for $\iota(0) = 1.49$, 1.50 and 1.51 respectively. The investigations with relative strong shear NM iota profiles with varied ι_{min} have confirmed the appearance of same mode for each iota profile. In simulations, the mode (m = 7, n = 10/11) appears for all of the seven strong shear NM iota profiles radially localized around $\rho = 0.45$ which is the location of ι_{min} and the obtained frequencies with AE3D simulations are consistent with the frequencies calculated through analytical dispersion relation using ι_{min}. This mode's consistency with similar NM iota profiles offers an opportunity to model the ι_{min} . **These calculations support the development of MHD spectroscopy as a sensitive iota profile diagnostic technique for the future fusion devices where**

other methods may not be practical due to high neutron flux.

The modes obtained in these calculations have global structures and therefore can be considered to impact the fast ion confinement and hence their heating efficiency. In modes analysis some cases show modulational effects of multiple competing Alfvén modes having discrete frequencies. Modes with lower frequency and radially extended global structures are characterized as GAEs and radially localized ones with relatively higher frequency as RSAEs. The width of mode (m = 7, n = 10/11) increases with the increase in ι_{min} values, therefore with the strong magnetic shear the mode becomes narrower and its frequency in each block of ι_{min} nearly remains constant which suggests the mode's growth rate reduces. Since a narrower mode has lower region for the interaction with energetic particles, it will tend to reduce the radial transport of the energetic particles. In conclusion, an iota profile with strong shear and lower ι_{min} is more favourable for the stability of Alfvénic instabilities in the TJ-II plasmas.

In future there is possibility of investigating these instabilities with the interaction of energetic particles by calculating their growth rates, amplitudes and three dimensional mode structures. Further investigations for the mode structures are possible for the low-frequency modes with the use of Alfvénic-acoustic coupling model in the AE3D code.

Acknowledgements

This work has been carried out within the framework of the EUROfusion Consortium and has received funding from the Euratom research and training programme 2014-2018 and 2019-2020 under grant agreement No 633053. The views and opinions expressed herein do not necessarily reflect those of the European Commission. Allah Rakha is grateful to 'AGAUR FI predoctoral grant' for supporting his PhD studies. This work has received funding from the Spanish Ministry of Economy and Competitiveness (MINECO) under grant ENE2015-67371-R. The work of AVM was supported by Russian Science Foundation (project 14-22-00193) and also was partly supported by the Competitiveness Programme of NRNU MEPhI.

References

[1] Wong K. L. *et al* 2004 *Phys. Rev. Lett.* **93** 085002
[2] Berk H. L. *et al* 2001 *Phys. Rev. Lett.* **87** 185002
[3] Sharapov S. E. *et al* 2002 *Phys. Plasmas* **9** 2027
[4] Breizman B. N. *et al* 2003 *Phys. Plasmas* **10** 3649
[5] Austin M. E. *et al* 2006 *Phys. Plasmas* **13** 082502
[6] Spong D. A. 2012 *Phys. Plasmas* **19** 082511
[7] Van Zeeland M. A. *et al* 2008 *Plasma Phys. Control. Fusion* **50** 035009
[8] Sharapov S. E. *et al* 2001 *Phys. Lett.* A **289** (3) 127
[9] Fasoli A. *et al* 2002 *Plasma Phys. Control. Fusion* **44** B159-B172
[10] Sharapov S. E. *et al* 2006 *Nucl. Fusion* **46** S868
[11] Sharapov S. E. *et al* 2018 *Nucl. Fusion* **58** 082008
[12] Toi K. *et al* 2010 *Phys. Rev. Lett.* **105** 145003

[13] Toi K. *et al* 2011 *Plasma Phys. Control. Fusion* **53** 024008
[14] Spong D. A. 2013 *Nucl. Fusion* **53** 053008
[15] Evans T. E. *et al* 1984 *Phys. Rev. Lett.* **53** 1743
[16] Kramer G.J. *et al* 2016 *Plasma Phys. Control. Fusion* **58** 085003
[17] Cooper W. A. *et al* 2010 *Phys. Rev. Lett.* **105** 035003
[18] Cooper W. A. *et al* 2013 *Nucl. Fusion* **53** 073021
[19] Melnikov A.V. *et al* 2014 *Nucl. Fusion* **54** 123002
[20] Spong D. A. *et al* 2017 *Nucl. Fusion* **57** 086018
[21] Kruger S. E., Hegna C. C. and Callen J. D. 1998 *Phys. Plasmas* **5** 4169
[22] Hirshman S. P. and Whitson J. C. 1983 *Phys. Fluids* **26** 3553
[23] Rakha A.*et al* 2019 *Nucl. Fusion* **59** 056002
[24] Cook C. R. *et al* 2016 *Plasma Phys. Control. Fusion* **58** 054004
[25] Rakha A. *et al* 2018 Modelling of Alfvén cascades in NBI heated stellarator plasmas *45th EPS Conference on Plasma Physics, Prague, Czech Republic 2018.*
[26] Romero J.A. *et al* 2014 *Nucl. Fusion* **54** 043008
[27] Spong D. A., Sanchez R. and Weller A. 2003 *Phys. Plasmas* **10** 3217
[28] Salat A. and Tataronis J. A. 2001 *Phys. Plasmas* **8** 1207
[29] Spong D. A., D'Azevedo E. and Todo Y. 2010 *Phys. Plasmas* **17** 022106
[30] Sleijpen G. L. G. and Van der Vorst H. A. 2000 *SIAM J. Matrix Anal. & Appl.***17** 401-425